


# Methodological framework for heart rate variability analysis during exercise: application to running and cycling stress testing

David Hernando<sup>1,2</sup>  · Alberto Hernando<sup>1,3</sup> · Jose A. Casajús<sup>4,5,6</sup> · Pablo Laguna<sup>1,2</sup> · Nuria Garatachea<sup>4,5,6</sup> · Raquel Bailón<sup>1,2</sup>

Received: 15 February 2017 / Accepted: 10 September 2017 / Published online: 26 September 2017  
© International Federation for Medical and Biological Engineering 2017

**Abstract** Standard methodologies of heart rate variability analysis and physiological interpretation as a marker of autonomic nervous system condition have been largely published at rest, but not so much during exercise. A methodological framework for heart rate variability (HRV) analysis during exercise is proposed, which deals with the non-stationary nature of HRV during exercise, includes respiratory information, and identifies and corrects spectral components related to cardiocomotor coupling (CC). This is applied to 23 male subjects who underwent different

tests: maximal and submaximal, running and cycling; where the ECG, respiratory frequency and oxygen consumption were simultaneously recorded. High-frequency (HF) power results largely modified from estimations with the standard fixed band to those obtained with the proposed methodology. For medium and high levels of exercise and recovery, HF power results in a 20 to 40% increase. When cycling, HF power increases around 40% with respect to running, while CC power is around 20% stronger in running.

**Keywords** Cardiocomotor coupling · Stride cadence · Pedalling cadence · Non-stationary analysis

---

✉ David Hernando  
dhernand@unizar.es

Alberto Hernando  
ahersanz@unizar.es

Jose A. Casajús  
joseant@unizar.es

Pablo Laguna  
laguna@unizar.es

Nuria Garatachea  
nugarata@unizar.es

Raquel Bailón  
rbailon@unizar.es

<sup>1</sup> Biomedical Signal Interpretation, Computational Simulation (BSICoS) Group at the Aragón Institute of Engineering Research (I3A), IIS Aragón, University of Zaragoza, Zaragoza, Spain

<sup>2</sup> Bioingeniería, Biomateriales y Nanomedicina (CIBER-BBN), Centro de Investigación Biomédica en Red (CIBER), Zaragoza, Spain

<sup>3</sup> Centro Universitario de la Defensa (CUD), Academia General Militar (AGM), Zaragoza, Spain

## 1 Introduction

Heart rate variability (HRV) is considered a non-invasive method to evaluate the condition of the autonomic nervous system (ANS) and its regulation over the heart. Spectral analysis of HRV at rest unveils at least two main components, which are located in a low-frequency (LF) band (0.04–0.15 Hz) and in a high-frequency (HF) band (usually measured at 0.15–0.4 Hz). Power in the LF band is

<sup>4</sup> Departamento de Fisiatría y Enfermería, Facultad de Ciencias de la Salud y del Deporte, GENUD (Growth, Exercise, Nutrition and Development) research group, Instituto Agroalimentario de Aragón IA2 (Universidad de Zaragoza-CITA), IIS Aragón, Zaragoza, Zaragoza, Spain

<sup>5</sup> Centro de Investigación Biomédica en Red de la Fisiopatología de la Obesidad y Nutrición (CIBEROBN), Zaragoza, Spain

<sup>6</sup> EXERNET, Red de Investigación en Ejercicio Físico y Salud para Poblaciones Especiales, Zaragoza, Spain

affected by both sympathetic and parasympathetic modulations together with other regulatory mechanisms such as the renin-angiotensin and baroreflex systems. Power in the HF band is synchronous with respiration and mainly influenced by the parasympathetic system. The ratio between the power in the LF and HF bands has been proposed to assess the sympathovagal balance controlling the heart rate (HR) (see Working Group of ESC [35] and Rajendra et al. [29]).

Standards of spectral analysis of HRV measurements, physiological interpretation and clinical use have largely been published at rest. However, HRV analysis during exercise testing is also appealing in sports sciences. Sports physiologists and trainers use HRV to understand autonomic changes due to exercise training and the cardiovascular response to the stress of exercise (Borresen et al. [7]), as well as a marker of overreaching or overtraining (Hottenrott et al. [15]). For physicians, HRV analysis during exercise allows to detect ANS alterations which may not be visible at rest, or that are more evident in those conditions, such as those induced by ischemia (Bailón et al. [5]). HRV analysis during recovery after exercise has also been used to predict risk of mortality (Pradhapan et al. [28]).

During an graded exercise test, HR and oxygen consumption rapidly increase in the beginning, following a slower increment afterwards. The increase in HR is the result of vagal withdrawal and sympathetic excitation (Sarmiento et al. [33]). There is also a significant drop in HRV in both LF and HF bands. As reported in Cottin et al. [9, 10] and Bailón et al. [1, 3], there is a reduction in the LF power with exercise. Power in HF band also decreases during moderate exercise [10], but during heavy exercise, HF power is said to be related to the mechanical effect of breathing on the sinus node, with increasing power with higher intensities of exercise (see Cottin et al [9, 11] and Blain et al. [6]). Still, HRV analysis and interpretation during exercise is challenging and a matter of debate.

One of the challenges in exercise HRV analysis is obtaining a reliable and robust QRS detection, mainly due to the significant noise levels observed in this context (Llamedo et al. [17]) and changes in beat morphology during exercise (Drezner et al. [12]). Several approaches have been proposed to deal with the non-stationary nature of HRV during exercise, like quadratic time-frequency representations, including the Wigner-Ville distribution and its filtered versions (Mainardi [18]; Orini et al. [26]). In order to separate changes in ANS stimulation from changes in mean HR, which greatly varies in exercise testing, a correction of HRV parameters with time-varying mean HR should be performed (see Bailón et al. [3], Meste et al. [23], and Sacha et al. [30, 32]). Respiratory rate also increases with increasing loads of exercise and can reach frequencies above the classic HF band, thus making necessary to redefine this band as shown in Bailón et al. [2], or adding respiratory frequency

information directly to the time-frequency estimation of HRV spectrum as shown in Bailón et al. [4]. Lastly, besides the LF and HF components, another component can appear in the HRV spectrum, which is synchronous with stride or pedalling frequency. This component can cause aliasing and may overlap with LF and HF bands, misleading their interpretation in terms of sympathetic or parasympathetic activation.

All these methodological issues have never been approached in an integrated manner. In this paper, we propose an integrated methodological framework for a robust HRV analysis during exercise. This framework will take into account all the former issues: correction by mean heart rate, time-frequency spectral analysis, redefinition of HF band based on respiratory frequency, and attenuation of the cardiocomotor coupling. Then, ANS response to exercise will be study through HRV analysis in different types of exercise, namely, maximal and submaximal, running and cycling.

## 2 Methods

### 2.1 Study population and experimental protocol

The database consists of 23 male volunteers. All of them were apparently healthy, they were not taking medications and they had normal blood pressure levels and electrocardiographic patterns. They regularly participated in sports activities, doing at least 3 days/week of regular aerobic training. Written informed consent was obtained from each subject. The study protocol was approved by the institutional ethics committee and was in accordance with the Declaration of Helsinki for Human Research of 1974 (last modified in 2013). Table 1 shows the study population characteristics.

All the subjects completed three sessions in consecutive weeks: a maximal test (on a treadmill) and two submaximal tests (on a treadmill and on a cycle ergometer), denoted as MaxT, SubT and SubC, respectively. The volunteers were asked to (1) wear comfortable, loose-fitting clothing; (2) drink plenty of fluids over the 24-h period preceding the test;

**Table 1** Study population characteristics (23 male volunteers): age, height, mass, body mass index and maximum oxygen consumption ( $\dot{V}O_2$  max). Mean  $\pm$  standard deviation

Age (years)	34.8 $\pm$ 5.0
Height (cm)	178.4 $\pm$ 5.7
Mass (kg)	74.8 $\pm$ 7.8
Body mass index ( $\text{kg} \cdot \text{m}^{-2}$ )	23.5 $\pm$ 2.5
$\dot{V}O_2$ max ( $\text{ml}O_2 \cdot \text{min}^{-1}$ )	4216.6 $\pm$ 453.7
$\dot{V}O_2$ max $\cdot \text{kg}^{-1}$ ( $\text{ml}O_2 \cdot \text{min}^{-1} \cdot \text{kg}^{-1}$ )	56.4 $\pm$ 6.2

(3) avoid food, tobacco, alcohol and caffeine for 3 h prior to the test; (4) avoid exercise or strenuous physical activity on the day of the test and (5) get an adequate amount of sleep (6–8 h) the night before the test, as proposed by Wasserman [34].

All tests were divided into three different phases: resting, exercise and recovery phase. The resting phase was common to all tests: the subjects were monitored seated for 5 min at rest, without any movement or talking, to measure resting cardiorespiratory variables.

For the exercise phase during MaxT test, the subjects performed an incremental maximal test to exhaustion on a motorized treadmill (Quasar Med 4.0, h/p/cosmos, Nussdorf-Traunstein, Germany). They began running with an initial speed of  $8 \text{ km} \cdot \text{h}^{-1}$  and increased  $1 \text{ km} \cdot \text{h}^{-1}$  every minute until the subjects stopped due to volitional exhaustion. From this test, the maximum HR and  $\dot{V}O_2$  were noted for each subject. A physician was present during the whole session supervising the test.

For the SubC test, the exercise started at 75 W on the cycle ergometer, increasing  $25 \text{ W} \cdot \text{min}^{-1}$ . The cadence frequency was fixed at 80 rpm. This phase continued until the subject reached his 90% maximum HR previously determined at the MaxT test, after that the load was kept for two more minutes. For the SubT test on the treadmill, the procedure was similar to the MaxT test, until they reached the 90% maximum HR, then they kept running two more minutes at that speed. Besides, in the SubT test, the running stride was fixed at  $80 \text{ strides} \cdot \text{min}^{-1}$ .

Recovery phase lasted between 3 and 5 min, where subjects were required to remain running at  $8 \text{ km} \cdot \text{h}^{-1}$  (on the treadmill) or pedalling at 75 W (on the cycle ergometer). However, subjects did not behave in a consistent way after the stress peak, especially in the MaxT test. Some subjects continued running at a slower speed but others completely interrupted the exercise and took some seconds until they could continue. For this reason, the first 30 s in this phase

will not be analysed. Figure 1 shows a flowchart for the experimental protocol.

### 2.2 Data acquisition and pre-processing

Information about respiratory frequency and oxygen consumption ( $\dot{V}O_2$ ) were obtained by an open-circuit sampling system (Oxycon Pro, Jaeger-Viasys Healthcare, Hoechberg, Germany). The metabolic cart was calibrated with a known gas mixture (16% oxygen,  $O_2$ , and 5% carbon dioxide,  $CO_2$ ) and volume prior to the first test each day as recommended by the company. Both respiratory frequency and  $\dot{V}O_2$  data were interpolated at 4 Hz and low-pass filtered with a cut-off frequency of 0.01 Hz to obtain  $f_R(n)$  and  $d\dot{V}O_2(n)$  series, respectively.

The ECG was recorded using a high-resolution Holter (Mortara 48-hour H12+, Mortara Instrument, Milwaukee, Wisconsin) with a sampling frequency of 1000 Hz. For each subject, the QRS detection marks were extracted from the ECG using a multi-lead approach by a wavelet-based detector described in Martínez et al. [20] with optimized parameters for noisy environments described in Hernando et al. [14], and each detection was manually verified by an operator with a dedicated interface. RR intervals from the ECG were obtained as the difference of each consecutive beat occurrences.

Thanks to a cadence sensor attached to the subject’s shoe (Polar s3 Stride Sensor, Polar Electro, Finland), the running stride frequency,  $f_C(n)$ , was obtained in the MaxT test, after low-pass filtering the raw data with a cut-off frequency of 0.01 Hz. In the submaximal tests, this component was fixed to the requested cadence ( $80 \text{ rpm} = 4/3 \text{ Hz}$ ).

Five intervals were established for each RR series for further analysis. In addition to the basal interval ( $I_B$ ), which is associated to the resting phase (5 min prior to the exercise), the  $d\dot{V}O_2(n)$  signal from the MaxT test was used to establish three intervals during the exercise: 0–60%, 60–80% and

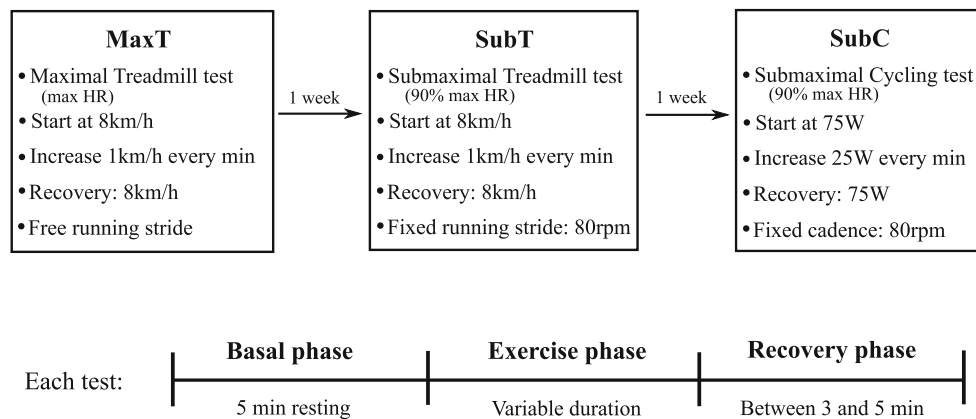
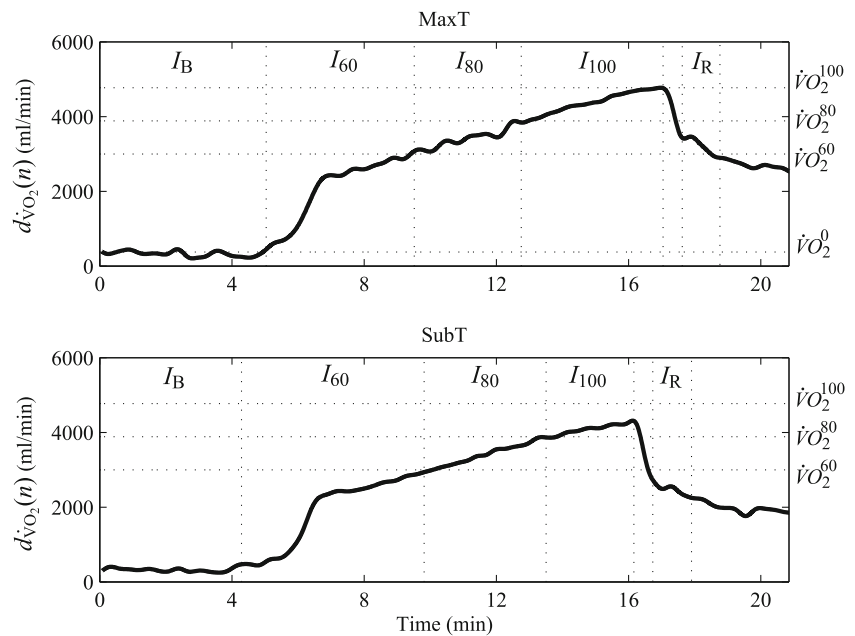


Fig. 1 Flowchart for the experimental protocol

**Fig. 2** Example of oxygen consumption signal in MaxT (upper panel) and SubT (lower panel) in intervals  $I_B$ ,  $I_{60}$ ,  $I_{80}$ ,  $I_{100}$  and  $I_R$  (basal phase, 0–60%, 60–80% and 80–100% of  $d\dot{V}O_2(n)$  defined by MaxT, respectively, and recovery phase) for one subject



80–100% of the variation between the basal ( $\dot{V}O_2^0$ ) and the maximum value ( $\dot{V}O_2^{100}$ ) of  $d\dot{V}O_2(n)$  during exercise for each subject (see Fig. 2, upper panel).  $\dot{V}O_2^0$  was obtained as the mean value of  $d\dot{V}O_2(n)$  during the resting phase, while  $\dot{V}O_2^{100}$  was found at the peak of  $d\dot{V}O_2(n)$ , both defined at the MaxT test. These intervals were denoted as  $I_{60}$ ,  $I_{80}$  and  $I_{100}$  respectively. The  $\dot{V}O_2$  threshold values found in the MaxT test were used also in the SubT and SubC tests to establish the intervals (see Fig. 2 (lower panel)). Since  $d\dot{V}O_2(n)$  in SubT and SubC do not reach  $\dot{V}O_2^{100}$ , the last interval (usually  $I_{100}$ ) lasts until the exercise phase ends. In four subjects, there is no  $I_{100}$  in SubC and their last interval is  $I_{80}$ . Note that each interval has different time length among the subjects. Additionally, the recovery interval ( $I_R$ ) starts 30 s after the peak of exercise and lasts for 1 min.

### 2.3 Heart rate variability estimation

The instantaneous heart rate signal,  $d_{HR}(n)$ , is derived from the QRS detection marks, following a method based on the integral pulse frequency modulation (IPFM) model, which also accounts for the presence of ectopic beats (Mateo et al. [21]). This method assumes that ANS activity can be modelled as a modulating signal  $m(n)$  which, together with a DC level, is integrated until it reaches a threshold  $T$ , when a beat occurs and the process is reset. The threshold  $T$  represents the mean interval length between successive beats when the DC level is set to one. The signal  $d_{HR}(n)$  is sampled at 4 Hz.

A low-pass filter is used to obtain the time-varying mean HR,  $d_{HRM}(n)$ , which contains the very low-frequency components, up to 0.04 Hz. Then, the HRV signal  $d_{HRV}(n)$  can be obtained as follows:

$$d_{HRV}(n) = d_{HR}(n) - d_{HRM}(n) \quad (1)$$

Still,  $d_{HRV}(n)$  is affected by changes in  $m(n)$  as well as in  $d_{HRM}(n)$ . To avoid measuring changes in  $d_{HRV}(n)$  which are due to changes in mean HR rather than to changes in the ANS modulation, the HRV signal has been proven to require a normalization by the time-varying mean HR (see Bailón et al. [3]), obtaining an estimation of the modulating signal,  $\hat{m}(n)$ , as follows:

$$\hat{m}(n) = \frac{d_{HRV}(n)}{d_{HRM}(n)} \quad (2)$$

### 2.4 Spectral components' definition

The smoothed pseudo Wigner-Ville distribution (SPWVD) is applied to  $\hat{m}(n)$  to estimate the instantaneous power spectrum of the HRV signal (Martin et al. [19]). To attenuate the interference terms, both time and frequency smoothing windows were chosen to be Hamming windows of length  $2N-1 = 203$  (about 50 s) and  $2K-1 = 513$  samples (about 128 s), respectively (Bailón et al. [1]).

There are three main spectral components which will be analysed. First, the instantaneous power in the LF band is extracted throughout the entire exercise test, denoted as  $P_{LF}(n)$ , integrating the instantaneous power of the time-frequency spectrum of  $\hat{m}(n)$  in the range from 0.04 to 0.15 Hz. Second,  $P_{HF}(n)$  is obtained using a time-varying HF band: this band is centred on  $f_R(n)$  with a bandwidth of 0.125 Hz; in this database, this HF band has resulted to be always above 0.15 Hz (no overlapping with the LF band) and below half the mean HR rate, (no aliasing is produced) (see Laguna et al. [16]).

Lastly, the third spectral component,  $P_{CF}(n)$ , is related to the cadence frequency component (CF). The band for

this component is centred at the running stride or pedalling frequency,  $f_C(n)$ , with a bandwidth of 0.125 Hz, its upper bound limited by half the mean HR. This frequency is fixed at 80 strides · min<sup>-1</sup> for the SubT test and at 80rpm for the SubC test, and varying in the MaxT test, as explained before.

The intrinsic sampling frequency of HRV is the HR. Whenever the CF component exceeds half the mean HR, aliased components appear in the visible part of the spectrum and can overlap with other bands (Bailón et al. [1]). Moreover, if the CF component is not a perfect sinusoid, it will contain harmonics in the multiples of the frequency where CF appears. These harmonics also produce alias. Two main aliased components appear in this database (see Fig. 3a). The aliased components are denoted as AF1 and AF2, and their powers are denoted as follows:

- $P_{AF1}(n)$ : in a band centered at  $d_{HRM}(n) - f_C(n)$  with a bandwidth of 0.125 Hz.
- $P_{AF2}(n)$ : in a band centered at  $-d_{HRM}(n) + 2 \cdot f_C(n)$  with a bandwidth of 0.125 Hz.

Note that  $P_{CF}(n)$  is obtained integrating the instantaneous power of the spectrum of  $\hat{m}(n)$  in the band centered at  $f_C(n)$ , but only up to half the mean HR rate. When  $f_C(n)$  exceeds it ( $P_{AF1}(n)$  appears in the visible spectrum),  $P_{CF}(n)$  is considered to be 0. In the same way, when  $f_C(n)$  is below half the mean HR rate, AF1 component does not appear.

Figure 3b shows an example of a time-frequency map showing some of the spectral components of HRV (HF, CF, AF1 and AF2), as well as an overlapping between HF and AF1 and AF2.

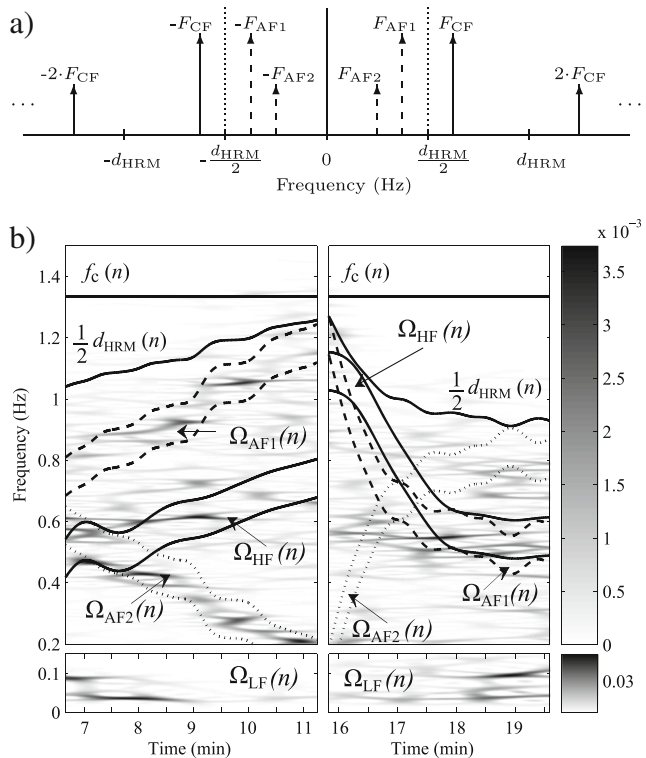


Fig. 3 Spectral components

AF1 and AF2), as well as an overlapping between HF and AF1 and AF2.

### 2.5 Overlapping effect attenuation

While measuring the HF power, there may be overlapping zones with other components, as seen in Fig. 3b. If an overlapping happens, the measured power reflects an artificial increase which should be corrected. Hence, several parameters are proposed to quantify the overlapping:

$$\alpha_{A,B}(n) = \frac{P_B(n)}{P_A(n) + P_B(n)}, \quad A, B \in \{HF, AF1, AF2\} \quad (3)$$

$$p_{A,B}(n) = \frac{\Omega_{A,B}(n)}{\Omega_B(n)}, \quad A, B \in \{HF, AF1, AF2\} \quad (4)$$

Where parameter  $\alpha_{A,B}(n)$  represents the dominance of  $P_B(n)$  with respect to  $P_A(n)$ , while parameter  $p_{A,B}(n)$  measures the ratio between the overlapped bandwidth between spectral components  $A$  and  $B$  ( $\Omega_{A,B}(n)$ ) and the  $B$  bandwidth ( $\Omega_B(n)$ ). The subindices  $A$  and  $B$  represent the components HF, AF1 and AF2. LF is not considered since  $\alpha_{LF,B}(n)$  is always nearly zero. This means that the considered aliased components have much less power than the LF component; thus, the LF correction is not necessary.

Whenever there is an overlapping between spectral components, which is measured by parameter  $p_{A,B}(n)$ ,  $\alpha_{A,B}(n)$  is used to compare both powers during 1 min prior to the overlapping. Hence, a time-varying  $M$ -sample mean signal,  $\bar{\alpha}_{A,B}(n)$ , is defined as follows:

$$\bar{\alpha}_{A,B}(n) = \begin{cases} \frac{1}{M} \sum_{k=n-M+1}^n \alpha_{A,B}(k) & \text{if } p_{A,B}(n) = 0 \\ \bar{\alpha}_{A,B}(n-1) & \text{if } p_{A,B}(n) \neq 0 \end{cases} \quad (5)$$

with  $M$  being the number of samples equivalent to 1 min ( $M = 240$  samples). Whenever an overlapping happens ( $p_{A,B}(n) \neq 0$ ), this dominance parameter does not update, maintaining the previous value, and thus avoiding errors in dominance estimation due to the overlapping. Note that this formula is valid if the overlapping happens at least 1 min after the beginning of the recording, which is always the case in this database.

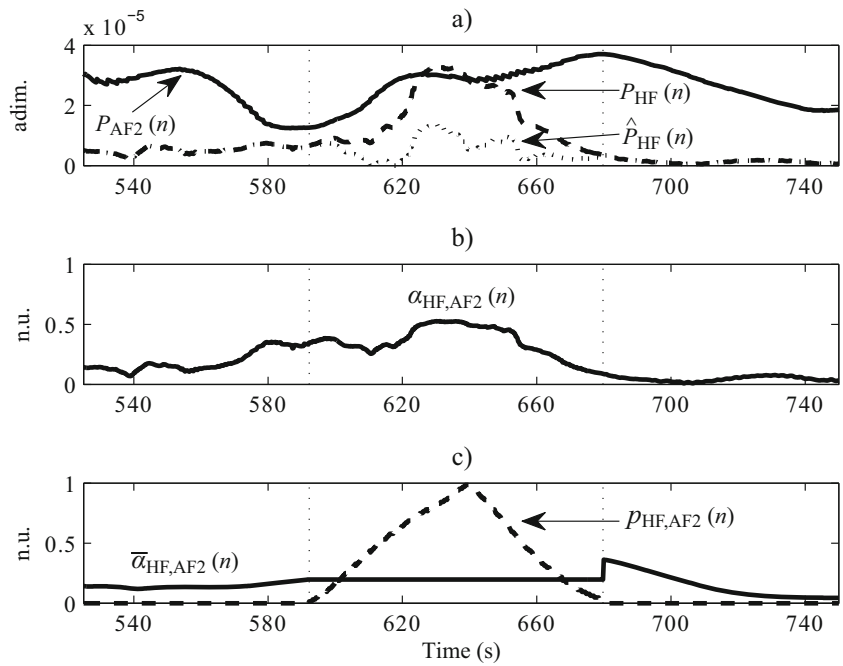
Then, the corrected power is estimated as follows:

$$\hat{P}_A(n) = P_A(n) - \sum_{B \neq A} \bar{\alpha}_{A,B}(n) \cdot p_{A,B}(n) \cdot P_B(n) \quad (6)$$

Figure 4 shows an example of HF power correction. Panel a shows  $P_{HF}(n)$  (blue) and  $P_{AF2}(n)$  (black), with the overlapping area marked with red dotted lines. Panel b shows  $\alpha_{HF,AF2}(n)$ . Panel c shows  $\bar{\alpha}_{HF,AF2}(n)$  (blue) and  $P_{HF,AF2}(n)$  (red). With these parameters,  $\hat{P}_{HF}(n)$  is obtained and showed in panel a (dashed blue).

Two more parameters,  $T_{ov}$  and  $S_{ov}$ , are defined to measure the duration and severity of an overlap for each subject

**Fig. 4** **a**  $P_{HF}(n)$  (dashed),  $P_{AF2}(n)$  and  $\hat{P}_{HF}(n)$  (dotted). **b**  $\alpha_{HF,AF2}(n)$ . **c**  $\bar{\alpha}_{HF,AF2}(n)$  and  $p_{HF,AF2}(n)$  (dashed). Vertical dotted lines delimit the overlapping area in all panels



and for each type of test. First,  $T_{A,B}$  and  $S_{A,B}$  are defined:  $T_{A,B}$  measures the fraction of time that an overlap between the  $A$  and  $B$  components lasts ( $p_{A,B}(n) \neq 0$ ), and  $S_{A,B}$  measures the severity of an overlap between the  $A$  and  $B$  components and is obtained as follows:

$$S_{A,B} = \frac{1}{N_{A,B}} \sum_n \bar{\alpha}_{A,B}(n) \cdot p_{A,B}(n) \tag{7}$$

where  $N_{A,B}$  denotes the length (in samples) of the overlap. Then,  $T_{ov}$  and  $S_{ov}$  are obtained as the mean value of  $T_{AF1,HF}$

and  $T_{AF2,HF}$ , and  $S_{AF1,HF}$  and  $S_{AF2,HF}$ , respectively, for each subject.

**2.6 Physiological indices**

To denote the power related to cardiocomotor coupling (CC) in a general way, we will use  $\hat{P}_{CC}(n)$  from here onwards. This is obtained as follows:

$$\hat{P}_{CC}(n) = P_{CF}(n) + \hat{P}_{AF1}(n) + \hat{P}_{AF2}(n) \tag{8}$$

**Fig. 5** Median and MAD of  $\bar{P}_{LF}^1$  (left panel) and  $\bar{P}_{HF}^1$  (right panel) in intervals  $I_B$ ,  $I_{60}$ ,  $I_{80}$ ,  $I_{100}$  and  $I_R$  (basal phase, 0–60%, 60–80% and 80–100% of  $d_{VO_2}(n)$ , respectively, and recovery phase) for the MaxT test. Brackets denote significant differences ( $p$  value < 0.05)

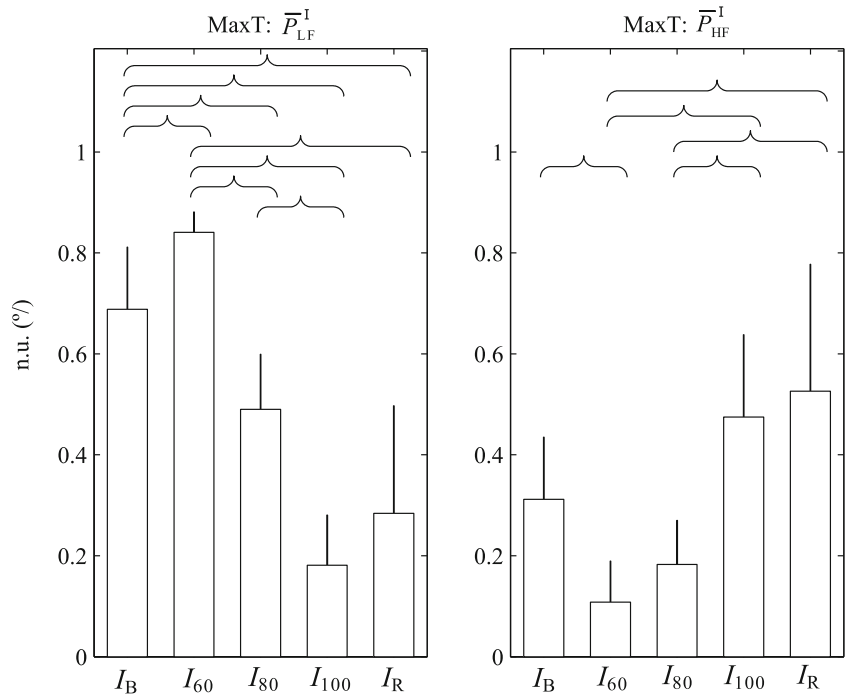
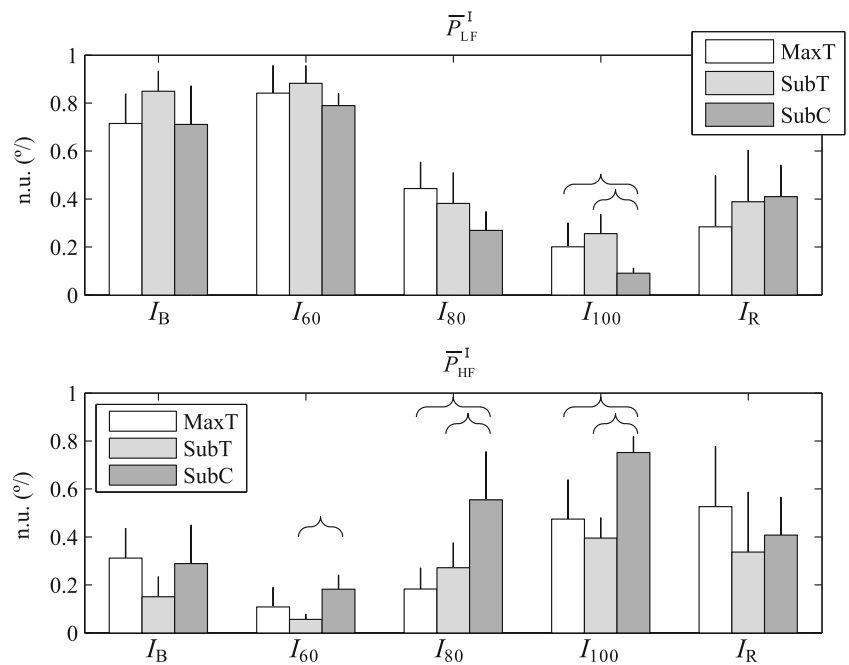


**Fig. 6** Median and MAD of  $\bar{P}_{LF}^I$  (upper panel) and  $\bar{P}_{HF}^I$  (lower panel) in intervals  $I_B$ ,  $I_{60}$ ,  $I_{80}$ ,  $I_{100}$  and  $I_R$  (basal phase, 0–60%, 60–80% and 80–100% of  $d_{\dot{V}O_2}(n)$  defined by MaxT, respectively, and recovery phase) for the MaxT, SubT and SubC tests. Brackets denote significant differences ( $p$  value < 0.05)



Due to the large changes of the total power for all bands, each instantaneous power is normalized by the instantaneous total power, which is defined as follows:

$$P_{TOT}(n) = P_{LF}(n) + \hat{P}_{HF}(n) + \hat{P}_{CC}(n) \tag{9}$$

Then, the studied power parameters are as follows:

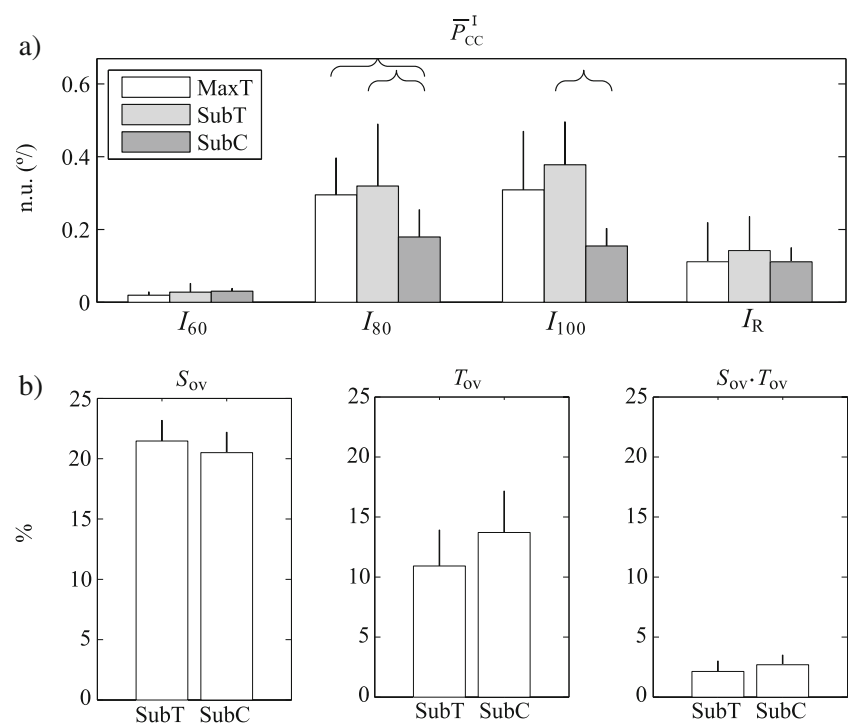
$$\bar{P}_{\mathcal{A}}^I = \frac{1}{N_I} \sum_{n \in I} \frac{\hat{P}_{\mathcal{A}}(n)}{P_{TOT}(n)}, \quad I \in \{I_B, I_{60}, I_{80}, I_{100}, I_R\} \tag{10}$$

where  $N_I$  denotes the length of the interval  $I$ , and the subindex  $\mathcal{A}$  indicates the chosen spectral component. Note that  $\bar{P}_{CC}^I$  is an exception and is not defined, since at rest there is no power related to cardiocomotor coupling.

The mean values of  $d_{HRM}(n)$ ,  $f_R(n)$  and  $d_{\dot{V}O_2}(n)$  are also obtained for each interval as follows:

$$\bar{d}_{HRM}^I = \frac{1}{N_I} \sum_{n \in I} d_{HRM}(n), \quad I \in \{I_B, I_{60}, I_{80}, I_{100}, I_R\} \tag{11}$$

**Fig. 7 a** Median and MAD of  $\bar{P}_{CC}^I$  in intervals  $I_B$ ,  $I_{60}$ ,  $I_{80}$ ,  $I_{100}$  and  $I_R$  (basal phase, 0–60%, 60–80% and 80–100% of  $d_{\dot{V}O_2}(n)$  defined by MaxT, respectively, and recovery phase) for the MaxT, SubT and SubC tests. Brackets denote significant differences ( $p$  value < 0.05). **b** Median and MAD of  $S_{ov}$  (left),  $T_{ov}$  (middle) and the product  $S_{ov} \cdot T_{ov}$  (right) for the SubT and SubC tests



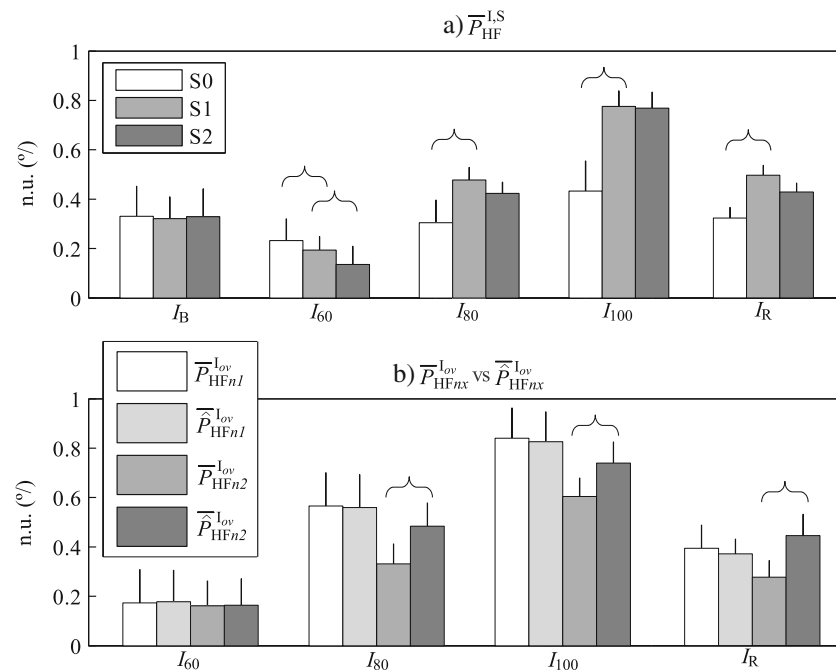


**Fig. 8** **a** Median and MAD of the evolution of  $\overline{P}_{HF}^{I,S}$  for the SubC test. Three different scenarios are shown: S0 (classical HRV analysis), S1 (S0 + redefinition of HF band based on  $f_R(n)$ ) and S2 (S1 + mean HR correction). **b** Median and MAD of  $\overline{P}_{HFnx}^{I,ov}$  (pre overlapping correction) and  $\overline{P}_{HFnx}^{I,ov}$  (post overlapping correction) for the SubC test when

CC components are considered. Two different normalizations are presented: only LF and HF components ( $HF_{n1}$ ), and total power including CC components ( $HF_{n2}$ ). Intervals  $I_B$ ,  $I_{60}$ ,  $I_{80}$ ,  $I_{100}$  and  $I_R$  refer to basal phase, 0–60%, 60–80% and 80–100% of  $d_{\dot{V}O_2}(n)$  defined by MaxT, respectively, and recovery phase. Brackets denote significant differences ( $p$  value < 0.05)

$$\overline{f}_R^I = \frac{1}{N_I} \sum_{n \in I} f_R(n), \quad I \in \{I_B, I_{60}, I_{80}, I_{100}, I_R\} \quad (12)$$

$$\overline{d}_{\dot{V}O_2}^I = \frac{1}{N_I} \sum_{n \in I} d_{\dot{V}O_2}(n), \quad I \in \{I_B, I_{60}, I_{80}, I_{100}, I_R\} \quad (13)$$

## 2.7 Statistical analysis

The Kolmogorov-Smirnov test showed that all  $\overline{P}_A^I$ ,  $\overline{d}_{HRM}^I$ ,  $\overline{f}_R^I$  and  $\overline{d}_{\dot{V}O_2}^I$  did not follow a normal distribution. Therefore, a Friedman test is applied for every parameter, followed by post hoc comparisons to study the differences between the different intervals within the same test, and between different tests. The difference is considered to be significantly different from zero when  $p < 0.05$ . Results in Figs. 5, 6, 7 and 8 are shown as median plus median absolute deviation (MAD) values.

## 3 Results

### 3.1 Characterization of the analysed intervals

Table 2 shows the mean and standard deviation of mean heart rate ( $\overline{d}_{HRM}^I$ ), respiratory frequency ( $\overline{f}_R^I$ ) and oxygen

consumption ( $\overline{d}_{\dot{V}O_2}^I$ ) in the different intervals for the three tests. Significant differences were found in  $I_{100}$  between MaxT and SubT in  $\overline{d}_{HRM}^I$  and  $\overline{f}_R^I$ , and between SubT and SubC in  $\overline{f}_R^I$ . In  $I_R$ , significant differences were found between MaxT and SubT in  $\overline{d}_{HRM}^I$  and  $\overline{f}_R^I$ , and between SubT and SubC in all the three parameters.

Table 3 shows the mean values of  $\hat{P}_{HF}$  and  $P_{TOT}$  in each interval and for each test in absolute units, i.e. without any normalization by  $P_{TOT}$ . A decreasing tendency can be observed in both powers with increasing intensities of the exercise (up to  $I_{100}$ ) and then they increase again in  $I_R$ .  $\hat{P}_{HF}$ , however, is slightly higher in  $I_{100}$  compared with  $I_{80}$  in MaxT and SubT.

### 3.2 Characterization of HRV indices in a maximal test

As it can be seen in Fig. 5,  $\overline{P}_{LF}^I$  increases at the beginning of the exercise ( $I_{60}$ ) with respect to the basal phase ( $I_B$ ), then it decreases again when the exercise load gets more intense, and increases in the recovery phase. Statistical analysis reveals that all intervals show significant differences with respect to  $\overline{P}_{LF}^{I_B}$  and  $\overline{P}_{LF}^{I_{60}}$  (see the brackets in Fig. 5). The opposite behaviour can be observed in  $\overline{P}_{HF}^I$ : it gets reduced at  $\overline{P}_{HF}^{I_{60}}$  and then it increases. However, it increases in the recovery phase. Significant differences can



**Table 2** Mean and std for mean heart rate ( $\bar{d}_{HRM}^I$ ), respiratory frequency ( $\bar{f}_R^I$ ) and oxygen consumption ( $\bar{d}_{VO_2}^I$ ) for the three tests: MaxT for maximal test on treadmill, SubT for submaximal test on treadmill and SubC for submaximal test on cycle ergometer

MaxT	$I_B$	$I_{60}$	$I_{80}$	$I_{100}$	$I_R$
$\bar{d}_{HRM}^I$ ( $s^{-1}$ )	1.09 ± 0.14	1.98 ± 0.19	2.51 ± 0.17	2.85 ± 0.14	2.71 ± 0.18
$\bar{f}_R^I$ (Hz)	0.24 ± 0.05	0.38 ± 0.08	0.51 ± 0.14	0.69 ± 0.14	0.67 ± 0.21
$\bar{d}_{VO_2}^I$ (ml $O_2 \cdot min^{-1}$ )	389.2 ± 50.2	1502.7 ± 390.1	2989.2 ± 298.5	3841.0 ± 442.6	3136.4 ± 880.3
SubT	$I_B$	$I_{60}$	$I_{80}$	$I_{100}$	$I_R$
$\bar{d}_{HRM}^I$ ( $s^{-1}$ )	1.04 ± 0.15	1.91 ± 0.15	2.40 ± 0.12	2.72 ± 0.12 *	2.56 ± 0.10 *†
$\bar{f}_R^I$ (Hz)	0.25 ± 0.04	0.40 ± 0.08 †	0.51 ± 0.12 †	0.65 ± 0.16 *†	0.61 ± 0.14 *†
$\bar{d}_{VO_2}^I$ (ml $O_2 \cdot min^{-1}$ )	418.1 ± 66.0	1643.0 ± 439.4	3059.4 ± 293.9	3805.1 ± 435.7	3406.3 ± 703.7 †
SubC	$I_B$	$I_{60}$	$I_{80}$	$I_{100}$	$I_R$
$\bar{d}_{HRM}^I$ ( $s^{-1}$ )	1.06 ± 0.18	1.86 ± 0.16	2.39 ± 0.17	2.70 ± 0.18	2.46 ± 0.11
$\bar{f}_R^I$ (Hz)	0.25 ± 0.07	0.36 ± 0.05	0.47 ± 0.08	0.58 ± 0.11	0.55 ± 0.15
$\bar{d}_{VO_2}^I$ (ml $O_2 \cdot min^{-1}$ )	423.3 ± 69.9	1637.2 ± 197.3	2964.6 ± 307.0	3612.4 ± 325.0	2573.2 ± 485.7

Different intervals are based of the oxygen consumption ( $\dot{V}O_2$ ):  $I_B$ ,  $I_{60}$ ,  $I_{80}$ ,  $I_{100}$  and  $I_R$  for the basal phase, 0–60%, 60–80% and 80–100% of  $\dot{V}O_2(n)$  defined by MaxT, respectively, and recovery phase. \* and † denote significant differences between MaxT and SubT, and between SubT and SubC, respectively ( $p$  value < 0.05)

be observed between  $\bar{P}_{HF}^{I_B}$  and  $\bar{P}_{HF}^{I_{60}}$ ,  $\bar{P}_{HF}^{I_{60}}$  and  $\bar{P}_{HF}^{I_{100}}$ ,  $\bar{P}_{HF}^{I_{100}}$  and  $\bar{P}_{HF}^{I_R}$ ,  $\bar{P}_{HF}^{I_R}$  and  $\bar{P}_{HF}^{I_{80}}$ , and  $\bar{P}_{HF}^{I_{80}}$  and  $\bar{P}_{HF}^{I_{60}}$ .

**3.3 Comparison between HRV indices in the submaximal tests and the maximal test**

Figure 6 shows  $\bar{P}_{LF}^I$  and  $\bar{P}_{HF}^I$  for the three tests in all intervals. The trending is similar for all the tests. Significant differences can be found in  $\bar{P}_{LF}^{I_{100}}$  in SubC test with respect to the other two tests.  $\bar{P}_{HF}^I$  in SubC also shows differences with respect to SubT test during the exercise ( $I_{60}$  to  $I_{100}$ ) and with respect to MaxT in  $I_{80}$  and  $I_{100}$ . No significant differences were found in  $I_R$ .

**3.4 Characterization of the cardiocomotor coupling**

Figure 7a shows  $\bar{P}_{CC}^I$  for the three tests in the exercise intervals ( $\bar{P}_{CC}^{I_B}$  is not defined). At the beginning of the exercise,

$\bar{P}_{CC}^I$  represents less than 10% of the total power. In the last two intervals of exercise, it reaches 20–30% of the total power. In the recovery phase, it represents about 10% of the total power.  $\bar{P}_{CC}^I$  in SubC is significantly different from SubT and MaxT in  $I_{80}$  and  $I_{100}$ . No differences were found in  $I_{60}$  and  $I_R$ .

Figure 7b shows different parameters to measure the severity of the overlaps. Only the two submaximal tests are compared (SubT and SubC), where  $f_C(n)$  was forced to be constant.  $S_{ov}$  is higher in SubT than SubC, which means that the power of the aliased components are higher in SubT with respect to the power in the HF band.  $T_{ov}$  is higher in SubC than SubT, which means that in SubT, the overlappings happen for a longer time than in SubC. Figure 7b also shows the product of  $S_{ov}$  and  $T_{ov}$ , which is very similar in both tests. No significant differences are found in those parameters.

**Table 3** Mean values of  $\hat{P}_{HF}$  and  $P_{TOT}$  in each interval and for each test in absolute units for the three tests: MaxT for maximal test on treadmill, SubT for submaximal test on treadmill and SubC for submaximal test on cycle ergometer

MaxT	$I_B$	$I_{60}$	$I_{80}$	$I_{100}$	$I_R$
$\hat{P}_{HF}$ ( $\times 10^{-5}$ ) (a.u.)	192.22	9.34	1.02	1.74	2.21
$P_{TOT}$ ( $\times 10^{-5}$ ) (a.u.)	509.38	64.91	11.02	3.82	11.35
SubT	$I_B$	$I_{60}$	$I_{80}$	$I_{100}$	$I_R$
$\hat{P}_{HF}$ ( $\times 10^{-5}$ ) (a.u.)	234.05	5.10	1.36	1.59	1.71
$P_{TOT}$ ( $\times 10^{-5}$ ) (a.u.)	624.18	125.17	5.73	3.88	9.62
SubC	$I_B$	$I_{60}$	$I_{80}$	$I_{100}$	$I_R$
$\hat{P}_{HF}$ ( $\times 10^{-5}$ ) (a.u.)	261.33	6.47	1.67	1.51	3.40
$P_{TOT}$ ( $\times 10^{-5}$ ) (a.u.)	745.34	37.19	5.33	2.64	14.98

Different intervals are based of the oxygen consumption ( $\dot{V}O_2$ ):  $I_B$ ,  $I_{60}$ ,  $I_{80}$ ,  $I_{100}$  and  $I_R$  for the basal phase, 0–60%, 60–80% and 80–100% of  $\dot{V}O_2(n)$  defined by MaxT, respectively, and recovery phase

### 3.5 Influence of each methodology step

Three main methodology aspects have been included in this work to address the problems due to the characteristics of exercise test HRV: (a) redefinition of HF band based on respiratory frequency, (b) mean HR correction of the HRV signal and (c) correction of the overlapped aliasing components related to CF. To study the influence of each of these methods, the evolution of normalized HF power was studied in different scenarios (reported here only for SubC), where different methodologies are applied step by step.

- Scenario 0 (S0): Classical HRV analysis is applied, i.e. HF band is fixed from 0.15 to 0.4 Hz, there is no mean HR correction and CF component is not considered.
- Scenario 1 (S1): The HF band is redefined based on  $f_R(n)$ .
- Scenario 1 (S2): In addition to S1, the mean HR correction is applied.
- Scenario 1 (S3): In addition to S2, the aliased components related to CF are attenuated. This is the framework used in the rest of the work.

Only the HF component is shown since LF does not change in S1 and S3. Moreover, since in S0–S2 the CF component is assumed not to exist, they will be studied separated from S3. Figure 8a shows the evolution of normalized HF power in S0 to S2. It is important to note that, only for this analysis, normalized power is obtained as follows:

$$\overline{P}_{\text{HF}}^{\text{I,S}} = \frac{1}{N_I} \sum_{n \in I} \frac{P_{\text{HF}}(n)}{P_{\text{LF}}(n) + P_{\text{HF}}(n)}, \quad S \in \{S0, S1, S2\} \quad (14)$$

since the CF component is not taken into account in the analysis, and thus, the measured powers are not comparable with those which are normalized by  $P_{\text{TOT}}(n)$ . Significant differences can be found in S1 for all exercise intervals, and in S2 in  $I_{60}$  (always with respect to the previous scenario).

Regarding the S3 scenario, CF component is identified, as well as its alias and the overlapping zones between CC and HF components. In this scenario,  $\overline{P}_{\text{HF}}^{\text{I}}$  is going to be redefined based on two different normalizations: only LF and HF components ( $\text{HF}_{n1}$ ), and total power including CC components ( $\text{HF}_{n2}$ ). The series  $P_{\text{HF}_{n1}}(n)$  and  $P_{\text{HF}_{n2}}(n)$ , and their corrected versions  $\hat{P}_{\text{HF}_{n1}}(n)$  and  $\hat{P}_{\text{HF}_{n2}}(n)$ , are obtained as follows:

$$P_{\text{HF}_{n1}}(n) = \frac{P_{\text{HF}}(n)}{P_{\text{LF}}(n) + P_{\text{HF}}(n)} \quad (15)$$

$$\hat{P}_{\text{HF}_{n1}}(n) = \frac{\hat{P}_{\text{HF}}(n)}{P_{\text{LF}}(n) + \hat{P}_{\text{HF}}(n)} \quad (16)$$

$$P_{\text{HF}_{n2}}(n) = \frac{P_{\text{HF}}(n)}{P_{\text{LF}}(n) + P_{\text{HF}}(n) + P_{\text{CF}}(n) + P_{\text{AF1}}(n) + P_{\text{AF2}}(n)} \quad (17)$$

$$\hat{P}_{\text{HF}_{n2}}(n) = \frac{\hat{P}_{\text{HF}}(n)}{P_{\text{LF}}(n) + \hat{P}_{\text{HF}}(n) + P_{\text{CF}}(n) + \hat{P}_{\text{AF1}}(n) + \hat{P}_{\text{AF2}}(n)} \quad (18)$$

Then, the mean value is obtained in each interval, taking into account only the overlapping zones:

$$\overline{P}_{\text{HF}_{nx}}^{\text{I}_{\text{ov}}} = \frac{1}{N_{\text{I}_{\text{ov}}}} \sum_{n \in I_{\text{ov}}} P_{\text{HF}_{nx}}(n) \quad (19)$$

$$\overline{\hat{P}}_{\text{HF}_{nx}}^{\text{I}_{\text{ov}}} = \frac{1}{N_{\text{I}_{\text{ov}}}} \sum_{n \in I_{\text{ov}}} \hat{P}_{\text{HF}_{nx}}(n) \quad (20)$$

where the subindex  $\text{HF}_{nx}$  denotes both normalizations  $\text{HF}_{n1}$  and  $\text{HF}_{n2}$ ,  $I_{\text{ov}}$  denotes the overlapping zones within each interval  $I$  ( $I \in \{I_{60}, I_{80}, I_{100}, I_R\}$ ) and  $N_{\text{I}_{\text{ov}}}$  denotes the length of the overlapping zones in the interval  $I$ .

Figure 8b shows changes in HF power during the overlapping zones in each interval, after attenuating any aliased components related to CF. Both normalizations are presented. In the first normalization, there are no significant differences after correction, with  $\overline{\hat{P}}_{\text{HF}_{n1}}^{\text{I}_{\text{ov}}}$  being slightly lower than  $\overline{P}_{\text{HF}_{n1}}^{\text{I}_{\text{ov}}}$  in  $I_{80}$  and  $I_{100}$ . In the second normalization,  $\overline{\hat{P}}_{\text{HF}_{n2}}^{\text{I}_{\text{ov}}}$  is significantly higher than  $\overline{P}_{\text{HF}_{n2}}^{\text{I}_{\text{ov}}}$  also in  $I_{80}, I_{100}$  and  $I_R$ , mainly because of the correction of the CC components. No differences are found in  $I_{60}$ .

## 4 Discussion

### 4.1 Methodological aspects

This work deals with analysing HRV in an exercise test database. Standard spectral analysis may fail to properly provide ANS information during exercise; hence, extra methodological steps should be taken into account. Most important challenges include a reliable and robust QRS detection, a proper method to deal with the non-stationary nature of HRV during exercise, removing the influence of the time-varying mean heart rate, adapting the HF band to the respiratory frequency, as well as taking care of additional spectral components which may interfere with the measurements.

The use of detector parameters optimized to noisy environments showed in [14] an improved combined performance (up to 19.36%) including sensitivity, positive predictivity and detection alignment when evaluating in a stress database.

The non-linear relation between heart rate and HRV has been previously addressed by mathematical models, in vivo experiments and animal models, and it has been proven than even in an innervated heart, there is a unique exponential decay-like relationship between HRV (measured by the SDNN) and intrinsic heart rate (see Monfredi et al. [25]). During an exercise test, there is a gradual dynamic change

in the mean heart rate which affects the LF and HF component estimation, as seen in Bailón et al. [3]. This dynamic mean heart rate may not correspond exactly with the intrinsic cardiac frequency but, we assume, is a valid surrogate of it. We use it to account for the mean heart rate influence on the LF and HF component estimation, in order not to overestimate or underestimate sympathetic and parasympathetic modulations, typically associated to the LF and HF bands, and thus have valid ANS markers irrespective of the heart rate. TVIPFM model, previously applied to heart rate variability analysis during exercise stress testing by Bailón et al. [1], is the underlying model used here to remove this mean heart rate influence. In this way, a continuous corrected HRV series can be obtained and HRV measurements at different mean heart periods can be safely compared. Chiu et al. [8] and Meste et al. [22] deal with this problem using a different methodology named the pulse frequency modulation model, which was also applied to obtain the continuous modulating signal. Sacha et al. [32] also address this problem and propose a method to weaken the influence of HR (Sacha et al. [30]) by dividing the RR interval tachograms or HRV spectra by the corresponding average RR intervals. This correction, however, should be performed not with the total average but with local averages in order not to lose the dynamic changes in an exercise test (Sacha et al. [31]).

Regarding the non-stationary nature of HRV during exercise, several tools have been proposed (see Mainardi [18]), such as short-time Fourier transform, time-varying autoregressive analysis and time-frequency representations. In this work, one of the existing time-frequency representations has been chosen, the smoothed pseudo Wigner-Ville distribution (SPWVD). Other studies (M. Orini et al. [27] and Chan et al. [8]) have validated the capability of this method to quantify HRV patterns in non-stationary conditions. The advantage of these methodologies is that they allow to define time-varying bands for the different spectral components. HF band has been defined centered at respiratory frequency since respiratory frequency increases with exercise intensity and can exceed the upper limit of classical HF band (0.4 Hz). HF bandwidth might be also dependent on respiratory spectra but in this work, a fixed band of 0.125 Hz has been used, since respiration spectra showed a very well defined and narrow peak around respiratory frequency.

The appearance of spectral components related to cardiocomotor coupling may lead to wrong interpretations of the state of ANS. Bailón et al. [1] already studied this component in the MaxT test with similar reports: it can reach around 30% of the total power. In a previous work, Hernando et al. [13] proposed a method to remove this component in the submaximal tests. This work proposes a generalization of that method to correct more than one overlapping zones between any two different components.

Regarding each methodological approach, four different scenarios have been studied: classical HRV analysis, the redefinition of HF band based on  $f_R(n)$  is added, the mean HR correction is added, and the attenuation of aliased components is added (see Fig. 8). At rest, there are no significant differences in the HF component in any scenario, since the mean heart rate does not significantly vary,  $f_R(n)$  is located within the classic HF band, and there is no CF component. Taking the classical HRV analysis as the reference, when the HF is located around  $f_R(n)$ , HF power is significantly different in all exercise intervals (around 5% lower in  $I_{60}$ , 20% higher in  $I_{80}$  and 40% higher in  $I_{100}$ ), since both HF bands start to differ at the beginning of the exercise when  $f_R(n)$  increases above the upper limit of the classic HF band (0.4 Hz), and maintains above it during the rest of the exercise. In the recovery phase, it is also higher when HF band is guided by respiration. In the next scenario, the mean HR correction is added, and there are significant differences only in  $I_{60}$ . In this interval, the mean HR greatly varies from the rest phase, while in  $I_{80}$  and  $I_{100}$ , the slope of mean HR is not as steep as in  $I_{60}$ .

In the last scenario, spectral components related to cardiocomotor coupling were identified and corrected when necessary. Two different normalizations have been studied. The first normalization,  $HF_{n1}$ , only takes into account LF and HF components. The second normalization,  $HF_{n2}$ , also includes cardiocomotor components. While  $HF_{n1}$  is commonly used in HRV analysis at rest as a measure of sympathovagal balance, HF component during moderate-to-high exercise intensities is no longer only related to ANS activity but also to a mechanical effect. This work proposes  $HF_{n2}$  to quantify the relative HF power with respect to all components found in HRV spectrum. Comparing pre- and post-overlapping correction in  $HF_{n1}$  during the overlappings, there are no significant differences.  $HF_{n2}$  prior to the correction shows lower values because both CC and HF components are contaminated. After correction, there are significant differences in  $I_{80}$ ,  $I_{100}$  and  $I_R$  in  $HF_{n2}$  with higher power (around 20% more) after the attenuation of the effect of cardiocomotor coupling. This effect is mainly due to the correction of the aliases of the CF component. However, the importance of this correction is more evident when each subject is studied separately. As an example, in Fig. 4, from seconds 600 to 650, HF power present a sudden increase, which could mislead the interpretation and relate it to a parasympathetic activation.

## 4.2 Physiological aspects

Heart rate variability power tends to decrease with exercise, which is shown in Table 3 and has been reported in previous works like in Sarmiento et al. [33]. Regarding the maximal test, which is presented as the reference

test, there is first a rapid increase of heart rate and oxygen consumption ( $I_{60}$ ). In this phase of moderate exercise, there is an increase in normalized LF power and a decrease in normalized HF power. This is mainly related with both a parasympathetic withdrawal and an augmented sympathetic activity, as suggested in Sarmiento et al. [33]. During moderate-to-high exercise intensities ( $I_{80}$  and  $I_{100}$ ), cardiac vagal control is no longer effective: in spite of the parasympathetic withdrawal, normalized HF power greatly increases due to the mechanical effect of breathing [33], which leads to a decrease of normalized LF power. When looking at the HF power in absolute units, this effect is not so apparent due to the overall reduction of HRV power, but still, HF power in  $I_{100}$  is slightly higher when compared to that in  $I_{80}$  in MaxT. Still, even after the power correction, respiratory sinus arrhythmia (i.e. HF power) is not a valid marker of parasympathetic activity during high intensities of exercise, being a limitation of HRV analysis during exercise.

There are no significant differences in the LF and HF power indices when comparing the two tests on the treadmill (MaxT and SubT). Looking at Fig. 7, it shows that CC power is always higher in SubT than MaxT. The reason may be that in MaxT, the cadence frequency was free, while in SubT it was fixed. Interestingly, the volunteers claimed that running at a fixed cadence during the incremental exercise did not feel natural. However, no significant differences were found in CC power between MaxT and SubT.

SubT and SubC are significantly different during exercise, mainly regarding HF power indices. LF power is only different in the last interval, near the peak of exercise. Millet et al. [24] state that central fatigue and decrease in maximal strength are more important after prolonged exercise in running than in cycling, which may impact in HRV parameters. They also claim that running exercise induces a higher oxygen uptake than cycling at the same intensity, being the metabolic demands different for each type of exercise. This also happens in this database, where  $\dot{V}O_2$  consumed in the last interval is always higher in SubT than that in SubC ( $3825.1 \pm 435.7$  vs  $3612.4 \pm 325.1$  ml  $O_2 \cdot kg^{-1} \cdot min^{-1}$ ). Moreover, four subjects did not reach the last interval in SubC because the maximum value of  $\dot{V}O_2$  in that test was lower than 80% of the max value in the MaxT test. However, the results of such physiological tests in cycling and running may be influenced by the athlete's original training background.

The largest differences between the submaximal tests can be found in CC power, where SubT presents higher levels of power than SubC. This component is related to cardiocomotor coupling, which might be due to the dynamic modulation of the venous return due to leg muscle contraction (Blain et al. [6]). Running may demand more power at muscle legs than cycling and so the effect of the arterial baroreceptors due to oscillations in venous return should

be stronger in SubT. This exercise test and their related CC power at HRV could provide useful information and have never been considered for quantification of the possible baroreflex sensitivity underlying this component, and eventually related to some pathologies related to this reflex. Another difference is that there is a reduction in the venous return during cycling compared to running, which may be due in part to peripheral muscle blood flow [24]. Moreover, subjects felt less natural to keep a fixed cadence while running on the treadmill than cycling and this additional effort may affect this component. These results suggest that this cardiocomotor component is less strong in cycle ergometer tests. No differences were found in the recovery phase when comparing the tests, but in MaxT and SubT, there is a significant decrease from  $I_{100}$  to  $I_R$ , while in SubC, there is no significant difference between those intervals.

Although no significant differences were found in the overlappings in SubT and SubC, it was found that  $S_{ov}$  was higher in SubT, while  $T_{ov}$  was higher in SubC. This means that the power in the aliased components is higher in SubT with respect to the HF power. However, this overlaps last shorter in SubT than SubC. If the overlapped areas are detected and removed from the study, it may be better to perform a test on a treadmill, where this overlaps are shorter. While on the other hand, if these overlaps are not detected, a test on a cycle ergometer may be preferred, since the severity of the overlaps is lower.

One limitation of this study is that the database is composed of only well-trained men subjects and so the results only apply for this type of population. This analysis should be extended also to women, and groups with different age and training level ranges to better understand how the ANS respond to the stress of exercise.

## 5 Conclusions

This work has proposed an integrated methodological framework for a robust HRV analysis during exercise. IPFM model allows to correct the HRV signal to remove the influence of the time-varying mean HR. Non-stationary nature of HRV during exercise has been solved by using the SPWVD, a time-frequency spectral analysis, which allows to extract continuous power information. HF band has been redefined and centered at the respiratory frequency. With this methodology, which mainly affects the HF measurements, HF power is increased in 20% during medium to high level of exercise, in 40% at peak exercise and in 20% at the recovery phase, being the more significant methodological step is the inclusion of respiratory information. Lastly, spectral components related to the stride/peddaling cadence have been identified and, whenever they overlapped with the

HF band, the measured powers have been corrected. When correcting these components, HF power is increased 20% during medium to high intensities of exercise and during recovery.

During the first phase of the exercise, there is a rapid increase of heart rate and oxygen consumption, together with an increase in normalized LF power and a decrease in normalized HF power. During moderate-to-high exercise intensities, however, there is an increase in normalized HF power despite the parasympathetic withdrawal, mainly due to the mechanical effect of breathing. In the recovery phase, an increase in normalized LF and a decrease in normalized HF are expected. When comparing running and cycling tests, normalized HF power differs, being around 20% greater while cycling. Power related to the stride/peddalling cadence during high intensities of exercise is around 15% stronger while running than cycling, being higher if this cadence is fixed.

**Acknowledgements** This work is supported by the CIBER in Bio-engineering, Biomaterials and Nanomedicine (CIBER-BBN) through Instituto de Salud Carlos III, by MINECO and FEDER under project TIN2014-53567-R, by Grupo Consolidado BSICoS ref:T96 from DGA and European Social Fund (EU). The computation was performed by the ICTS NANBIOSIS, more specifically by the High Performance Computing Unit of the CIBER-BBN at the University of Zaragoza.

## References

- Bailón R, Garatachea N, de la Iglesia I, Casajús JA, Laguna P (2013) Influence of running stride frequency in heart rate variability analysis during treadmill exercise testing. *IEEE Trans Biomed Eng* 60(7):1796–1805
- Bailón R, Laguna P, Mainardi L, Sörnmo L (2007) Analysis of heart rate variability using time-varying frequency bands based on respiratory frequency. In: 29th Annual International Conference of the IEEE Engineering in Medicine and Biology Society (EMBC07), vol 29, pp 6674–6677
- Bailón R, Laouini G, Grao C, Orini M, Laguna P, Meste O (2011) The integral pulse frequency modulation with time-varying threshold: application to heart rate variability analysis during exercise stress testing. *IEEE Trans Biomed Eng* 58(3):642–652
- Bailón R, Mainardi L, Orini M, Sörnmo L, Laguna P (2010) Analysis of heart rate variability during exercise stress testing using respiratory information. *Biomed Signal Process Control* 5:299–310
- Bailón R, Serrano P, Laguna P (2011) Influence of time-varying mean heart rate in coronary artery disease diagnostic performance of heart rate variability indices from exercise stress testing. *J Electrocardiol* 44:445–452
- Blain G, Meste O, Blain A, Bermon S (2009) Time–frequency analysis of heart rate variability reveals cardioloomotor coupling during dynamic cycling exercise in humans. *Amer J Physiol Heart Circ Physiol* 296:1651–1659
- Borresen J, Lambert M (2008) Autonomic control of heart rate during and after exercise: measurements and implications for monitoring training status. *Sports Med* 38(8):633–646
- Chan HL, Huang HH, Lin JL (2001) Time-frequency analysis of heart rate variability during transient segments. *Ann Biomed Eng* 29(11):983–996
- Cottin F, Médigue C, Leprêtre P, Papelier Y, Koralsztein J, Billat V (2004) Heart rate variability during exercise performed below and above ventilatory threshold. *Med Sci Sports Exerc* 36(4):594–600
- Cottin F, Papelier Y (2002) Regulation of cardiovascular system during dynamic exercise: integrative approach. *Crit Rev Phys Rehabil Med* 14(1):53–81
- Cottin F, Papelier Y (2008) Effect of heavy exercise on spectral baroreflex sensitivity, heart rate, and blood pressure variability in well-trained humans. *Amer J Physiol Heart Circ Physiol* 295:H1150–H1155
- Drezner JA, Fischbach P, Froelicher V, Marek J, Pelliccia A, Prutkin JM, Schmied CM, Sharma S, Wilson MG, Ackerman MJ, Anderson J, Ashley E, Asplund CA, Baggish AL, Brjesson M, Cannon BC, Corrado D, DiFiori JP, Harmon KG, Heidbuchel H, Owens DS, Paul S, Salerno JC, Stein R, Vetter VL (2013) Normal electrocardiographic findings: recognising physiological adaptations in athletes. *Br J Sports Med* 47(3):125–136
- Hernando A, Hernando D, Garatachea N, Casajús JA, Bailón R (2015) Attenuation of the influence of cardioloomotor coupling in heart rate variability interpretation during exercise test. In: 37th Annual International Conference of the IEEE EMBS: 1508–1511
- Hernando D, Bailón R, Almeida R, Hernández A (2014) QRS detection optimization in stress test recordings using evolutionary algorithms. *XLI International Conference on Computing in Cardiology: 737–740*
- Hottenrott K, Hoos O, Esperer H (2006) Heart rate variability and physical exercise. *Current Status Herz* 31(6):544–552
- Laguna P, Moody GB, Mark R (1998) Power spectral density of unevenly sampled data by least-square analysis. *IEEE Trans Biomed Eng* 45(6):698–715
- Llamedo M, Martínez JP (2014) QRS detectors performance comparison in public databases. *XLI International Conference on Computing in Cardiology: 357–360*
- Mainardi L (2009) On the quantification of heart rate variability spectral parameters using time–frequency and time-varying methods. *Philosophical Transactions of the Royal Society of London A: Mathematical. Phys Eng Sci* 367(1887):255–275
- Martin W, Flandrin P (1985) Wigner–Ville spectral analysis of nonstationary processes. *IEEE Trans Acoust Speech Signal Process* 33:1461–1470
- Martínez JP, Almeida R, Olmos S, Rocha AP, Laguna P (2004) A wavelet-based ECG delineator: evaluation on standard databases. *IEEE Trans Biomed Eng* 51(4):570–581
- Mateo J, Laguna P (2003) Analysis of heart rate variability in the presence of ectopic beats using the heart timing signal. *IEEE Trans Biomed Eng* 50(3):334–343
- Meste O, Khaddoumi B, Blain G, Bermon S (2005) Time-varying analysis methods and models for the respiratory and cardiac system coupling in graded exercise. *IEEE Trans Biomed Eng* 52(11):1921–1930
- Meste O, Rix H, Blain G (2009) ECG processing for exercise test. *Advanced Biosignal Processing*. Springer, Berlin
- Millet GP, Vleck VE, Bentley DJ (2009) Physiological differences between cycling and running: lessons from triathletes. *Sports Med* 39(3):179–206
- Monfredi O, Lyashkov AE, Johnsen AB, Inada S, Schneider H, Wang R, Nirmalan M, Wisloff U, Maltsev VA, Lakatta EG, Zhang H, Boyett MR (2014) Biophysical characterization of the underappreciated and important relationship between heart rate variability and heart rate. *Hypertension* 64(6):1334–1343
- Orini M, Bailón R, Enk R, Koelsch S, Mainardi L, Laguna P (2010) A method for continuously assessing the autonomic

- response to music-induced emotions through HRV analysis. *Med Biol Eng Comput* 48:423–433
27. Orini M, Bailón R, Mainardi L, Laguna P (2012) Synthesis of HRV signals characterized by predetermined time-frequency structure by means of time-varying ARMA models. *Biomed Signal Process Control* 7:141–150
  28. Pradhapan P, Tarvainen M, Nieminen T, Lehtinen R, Nikus K, Lehtimäki T, Kähönen M, Viik J (2014) Effect of heart rate correction on pre- and post-exercise heart rate variability to predict risk of mortality—an experimental study on the FINCAVAS cohort. *Front Physiol* 5:208. <https://doi.org/10.3389/fphys.2014.00208>
  29. Rajendra AU, Paul JK, Kannathal N, Lim C, Suri J (2006) Heart rate variability: a review. *Med Biol Eng Comput* 44:1031–1051
  30. Sacha J, Barabach S, Statkiewicz-Barabach G, Sacha K, Müller A, Piskorski J (2013) How to strengthen or weaken the HRV dependence on heart rate—description of the method and its perspectives. *Int J Cardiol* 168:1660–1663
  31. Sacha J, Pluta W (2005) Which heart rate is more variable: a slow or a fast one? It depends on the method of heart rate variability analysis. *Folia Cardiol* 12(suppl. D):1–4
  32. Sacha J, Pluta W (2008) Alterations of an average heart rate change heart rate variability due to mathematical reasons. *Int J Cardiol* 128:444–447
  33. Sarmiento S, García-Manso JM, Martín-González JM, Vaamonde D, Calderón J, Da Silva-Grigoletto ME (2013) Heart rate variability during high-intensity exercise. *J Syst Sci Complex* 26:104–116
  34. Wasserman K (2011) Principles of exercise testing and interpretation: including pathophysiology and clinical applications. Lippincott Williams & Wilkins, Philadelphia
  35. Working group of ESC (1996) Heart rate variability. standards of measurement, physiological interpretation, and clinical use. *Eur Heart J* 17:354–381

**David Hernando** is a PhD student in University of Zaragoza, Spain. His research interests include biomedical signal processing, focused in autonomic nervous system assessment through heart rate variability analysis.

**Alberto Hernando** works in Centro Universitario de la Defensa (CUD). His main research activity lies in the field of biomedical signal processing, focused in stress tests and mental disorders.

**Jose A Casajús** is Full Professor at the Universidad de Zaragoza. His research field is relationship with exercise, physical activity and health. He has co-authored over 140 research papers on Sport Science Area.

**Pablo Laguna** is Full Professor of Signal Processing, University of Zaragoza, Spain. He has co-authored over 130 research papers on biomedical signal processing and 250 international conference papers, and has advised 14 Ph.D Thesis.

**Nuria Garatachea** is Associate Professor of exercise physiology, Faculty of Health and Sport Science, University of Zaragoza. She has co-authored over 100 research papers on physical activity and health.

**Raquel Bailón** is Associate Professor of Signal Processing at the University of Zaragoza, Spain. Her current research interests include the biomedical signal processing field, specially in the analysis of the dynamics and interactions of cardiovascular signals.